The current issue and full text archive of this journal is available at
www.emeraldinsight.com/0961-5539.htm

Latent and sensible heat transfer in air-cooling applications

G. Comini and S. Savino
Dipartimento di Energetica e Macchine, University of Udine, Udine, Italy

Received 5 July 2006
Accepted 28 September 2006

Abstract

Purpose – Joint descriptions of both heat and mass transfer and thermodynamic aspects of air-cooling applications cannot be easily found in the literature. Numerical analyses are a notable exception since suitable physical models and realistic boundary conditions are a prerequisite of accurate simulations. Thus, it is believed that the experience gained with numerical simulations might be of some help also to designers of air-conditioning and drying systems. This paper seeks to address this issue.

Design/methodology/approach – In the text, the physical implications of governing equations and boundary conditions utilized in numerical simulations are extensively discussed. Particular attention is paid to the thermodynamically consistent definition of latent and sensible heat loads, and to the correct formulation of the heat and mass transfer analogy.

Findings – Comparisons of analytical and numerical results concerning forced flows of humid air over a cooled plate validate the assumptions made in numerical simulations, both for air-conditioning applications (almost always characterized by low rates of mass convection) and drying applications (almost always characterized by high rates of mass convection).

Originality/value – Finally, with reference to the cold plate problem investigated here, the effects of the suction flow induced by condensation on the Nusselt number are quantified.

Keywords Heat transfer, Convection, Drying, Cooling equipment, Numerical analysis

Paper type Research paper

Nomenclature

A = exchange area (m^2)
c_p = specific heat at constant pressure (kJ/(kg K))
$\mathscr{D}$ = diffusion coefficient (m^2/s)
g = gravity acceleration (kJ/kg)
G = chemical potential per unit mass (kJ/kg)
Δh = capillary depression (m)
H_{vl} = latent heat of condensation per unit mass (kJ/kg)
k = thermal conductivity (W/(m K))
L = length (m)
Le = Lewis number (= Sc/Pr)
$\dot{m}$ = mass flow rate (kg/s)
$\dot{m}''$ = mass flow rate per unit area (kg/(s m^2))
n = coordinate normal to the surface (m)
Nu = Nusselt number
Pr = Prandtl number
p = pressure (Pa)
q = heat flow rate (W)
q'' = heat flux (W/m^2)
r = radius (m)
Re_L = Reynolds number ($= \rho|\boldsymbol{v}_\infty|L/\mu$)
Sc = Schmidt number
Sh = Sherwood number
t = temperature (°C)
T = absolute temperature (K)
$\mathbf{v}$ = velocity vector (m/s)
v_τ, v_n = velocity components in the (τ, n) directions (m/s)
W = width (m)
x = humidity ratio (kg_{vapor}/kg_{dryair})

Greek symbols

α = contact angle
μ = viscosity (kg/(s m))
ρ = density (kg/m^3)
σ = surface tension (J/m^2)

International Journal of Numerical Methods for Heat & Fluid Flow
Vol. 17 No. 6, 2007
pp. 608-627
© Emerald Group Publishing Limited
0961-5539
DOI 10.1108/09615530710761234

τ = coordinate tangential to the surface (m)
ω = mass fraction of water vapor ($kg_{vapor}/kg_{humid\ air}$)

Subscripts
a = advective, air
d = diffusion
k = sensible
l = liquid
n = normal direction
v = vapor
s = saturation
w = wall
λ = latent
τ = tangential direction
∞ = free-stream value

Introduction

In many HVAC systems and in a great number of home and industrial appliances, transfers of latent and sensible heat occur simultaneously because of the condensation of water vapor on the exchange surfaces. Typical examples are heat exchangers used for summer air-conditioning operations (see Chapter 11 of Kuehn *et al.*, 1998), enthalpy exchangers utilized for dehumidification and total heat recovery (Spahier and Worek, 2004), and process-air dehumidifiers employed in textile driers, forced-convection ovens and dishwashers (Bari *et al.*, 2005). However, despite the sizable body of literature dealing with the prediction of latent and sensible fluxes under dehumidifying conditions, not much attention has been devoted to the development of models dealing with both heat and mass transfer and thermodynamic aspects of the processes investigated. To partially fill this gap, the illustration of successful procedures utilized routinely in numerical simulations might be of some help.

Conventionally, the vapor saturation pressure, and thus the dew-point temperature and the relative humidity of air, are defined with respect to a flat surface of water. In such a case the saturation, or equilibrium, vapor pressure is a function of temperature only. In reality, because of the surface tension, the saturation pressure is a function not only of temperature but also of the curvature of the interface. As shown in Appendix 1, highly curved surfaces have higher equilibrium vapor pressures than flat surfaces (Mitrovic, 2004; Galvin, 2005). Therefore, a very small droplet of water with large curvature will evaporate in an environment which, according to the conventional definition, is saturated. The smaller the droplet, the more pronounced this effect is since the saturation vapor pressure increases with decreasing droplet sizes. For a radius of the droplet approaching zero, the saturation pressure approaches infinity. As a consequence, homogeneous nucleation occurring within a humid air-stream is quite unlikely. On the contrary, heterogeneous nucleation appears frequently, since an incipient water droplet forming on a nucleus of condensation has much less curvature in relation to its mass. Nucleation on foreign particles, for example, occurs worldwide in the atmosphere and leads to the formation of cloud droplets (see Chapter 4 of Wallace and Hobbes, 1977). In cooling apparatuses, foreign particles are not usually present and, in general, condensation appears on the wall surfaces, where nucleation processes are facilitated by surface tension between solid and fluid and by small surface irregularities (Na and Webb, 2004). (A physical interpretation of the influences of contact angle and roughness on nucleation is presented in Appendix 1.) In accordance with the above considerations, numerical simulations assume that the air which comes into contact with a surface at a temperature below the dew-point, is first brought to the wall temperature, and only afterwards is dehumidified until the final equilibrium state is reached.

Accurate simulations of air-cooling processes require proper wall boundary conditions for the velocity components. Since, the late 1950s, the pioneering studies of Hartnett and Eckert have established that condensation and evaporation induce advective flows at the walls (Hartnett and Eckert, 1957; Eckert and Drake, 1959). In the case of condensation, advective velocities are directed towards the cooling surface, generating a suction effect which reduces the thickness of the boundary layer. In processes with low rates of mass convection, such as air-conditioning, the transverse flux of matter and the induced advective velocities are usually small and can be disregarded without significantly affecting the accuracy of the computations (Volchkov *et al.*, 2004). On the contrary, in processes with high rates of mass convection, such as drying, the advective velocities must be accounted for (Volchkov *et al.*, 2004). A key point of interest is whether the presence of non-zero advective velocities in correspondence with the cooling surface prevents, or not, the use of the analogy between heat and mass convection. According to Mills (1999), the validity of the analogy is limited to processes with low-rates of mass convection. On the other hand, a recently proposed formulation of the analogy seems to hold good for both low- and reasonably high-rates of mass convection (Volchkov *et al.*, 2004).

In principle, the modeling of cooling processes that involve adjacent fluid and solid domains requires the solution of a conjugate problem. However, conduction in the solid and convection in the fluid can often be decoupled by imposing constant temperature boundary conditions on the interface between the fluid and solid domains. If, in addition to being known, the interface temperature is lower than the dew point and the condensate is promptly removed from the exchange surfaces, the ideal gas relationship yields a constant value of the mass fraction of water vapor at the wall (corresponding to the saturation pressure at the wall temperature). Ignoring the presence of the condensed liquid has several justifications. First of all, designers always devote much effort to the achievement of a good drainage since retained condensate might either blow-off the heat exchanger, creating an unwanted fog, or remain on the cooling surface, providing a medium for the growth of bacteria (Korte and Jacobi, 2001). Furthermore, the influence of liquid droplets and films has not even been fully established experimentally (Korte and Jacobi, 2001; Hu *et al.*, 1994; Ramadhyani, 1998). The reason is that liquid droplets increase the effective roughness of the exchange surface. Thus, they increase friction factors and heat convection coefficients in turbulent flows, but not in laminar flows which are rather insensitive to roughness effects. Similarly, liquid films increase pressure losses and convection rates by increasing average axial velocities, but also bring about additional thermal resistances. The prevailing opinion is that the pressure loss is increased by the retained condensate, at least in the presence of liquid films, but it is still unclear whether the heat and mass convection coefficients are increased or decreased.

Despite the simplicity of decoupled formulations which disregard the presence of condensed liquid on the cooling surface, numerical modeling of simultaneous heat and mass transfer has not received much attention in the literature. However, with reference to laminar flows and boundary conditions of the first kind on the exchange surfaces, our research group recently analyzed decoupled heat and mass convection processes occurring simultaneously in a variety of tube-fin and plate-fin exchangers (Comini and Croce, 2001, 2003; Comini *et al.*, 2002). In these simulations, we neglected the advective velocities induced by condensation. In the present paper, on the contrary,

we take into account the effects of the advective velocities induced by condensation of water vapor in a forced flow of humid air over a cold plate.

The resulting problem is geometrically simple, but the governing equations are coupled through the wall boundary conditions for the Navier-Stokes equations. The non-zero advective velocities, in fact, modify the flow field and thus influence also the species and the energy conservation equations. Consequently, the solution must be based on an iterative procedure. In the presentation of results we favor the McQuinston (1975) approach, which deals with the ratio between sensible (q''_k) and total (q''_w) heat fluxes, rather than the Threlkeld's approach ((Kuehn *et al.*, 1998) pp. 309-311), which expresses the total heat flux in terms of enthalpy differences. The ratios q''_k/q''_w obtained from our numerical model are thus compared with the values yielded by the heat and mass transfer analogies illustrated in the text.

The proposed methodology leaves much room for further research. In particular, the effects on the Nusselt number of the suction flow induced by condensation must be quantified with reference, for example, to the correlations used for the prediction of convection coefficients. To this aim, some indications are provided for the cold plate problem investigated here.

Governing equations

For laminar flows of an incompressible, constant property fluid, the governing equations are the continuity and Navier-Stokes equations, the species conservation equation, and the energy equation (Comini and Cortella, 2005). The continuity and Navier-Stokes equations can be written as:

$$\nabla \cdot \mathbf{v} = 0 \tag{1}$$

and:

$$\rho \frac{\partial \mathbf{v}}{\partial \vartheta} + \rho \mathbf{v} \cdot \nabla \mathbf{v} = \mu \nabla^2 \mathbf{v} - \nabla p \tag{2}$$

respectively. The species conservation equation can be written as:

$$\frac{\partial \omega}{\partial \vartheta} + \mathbf{v} \cdot \nabla \omega = \mathscr{D} \nabla^2 \omega \tag{3}$$

In the absence of volumetric heating, by neglecting the effects of viscous dissipation and the energy transport connected with diffusion, the energy equation can be written as:

$$\rho c_p \frac{\partial t}{\partial \vartheta} + \rho c_p \mathbf{v} \cdot \nabla t = k \nabla^2 t \tag{4}$$

In the above equations ϑ is the time, p is the pressure, ω is the mass fraction of water vapor in the humid-air mixture, t is the temperature and the other properties and variables are defined as follows.

The density:

$$\rho = \rho_a + \rho_v \tag{5}$$

the viscosity:

$$\mu = (1 - \omega)\mu_a + \omega\mu_v \tag{6}$$

the specific heat at constant pressure:

$$c_p = (1 - \omega)c_{pa} + \omega c_{pv} \tag{7}$$

and the thermal conductivity k:

$$k = (1 - \omega)k_a + \omega k_v \tag{8}$$

are suitable combinations of dry-air and water-vapor values. In the calculations, the thermophysical properties are assumed to be constant and equal to their average values between the free-stream and the wall surface.

The velocity of the mixture is a mass-average:

$$\mathbf{v} = (1 - \omega)\mathbf{v}_a + \omega\mathbf{v}_v \tag{9}$$

between the dry-air velocity $\mathbf{v}_a$ and the water-vapor velocity $\mathbf{v}_v$. The binary mass diffusion coefficient $\mathscr{D}$ accounts for the molecular diffusion of water vapor into dry air. (Because of the reciprocity relation, however, the same value of the binary mass diffusion coefficient characterizes also the molecular diffusion of dry air into water vapor.) It is important to note that the species conservation equation is written for a medium which, locally, moves with the velocity $\mathbf{v}$. Consequently, the mass fluxes of water vapor referred to in equation (3), have two components: the advective component $\omega\mathbf{v}$, which represents the bulk transport of water vapor, and the diffusive component $\mathscr{D}\nabla\omega$, which represents the molecular transport of water vapor relative to a medium which moves with the mass average velocity $\mathbf{v}$ (Comini and Cortella, 2005).

To complete the formulation, appropriate boundary conditions must still be imposed. These conditions will be discussed in the following section, with reference to situations in which temperature and mass fractions have known values on the interfaces between fluid and solid domains.

Boundary conditions

Inflow, outflow and free-stream boundary conditions can be formulated in the usual way. At inflow we prescribe distributions of velocity, concentration and temperature which coincide with the conditions prevailing in the free-stream (denoted by the infinity subscript):

$$\mathbf{v} = \mathbf{v}_\infty; \quad \omega = \omega_\infty; \quad t = t_\infty \tag{10}$$

At outflow, we can assume fully developed distributions of velocity, concentration and temperature:

$$\frac{\partial \mathbf{v}}{\partial n} = \frac{\partial \omega}{\partial n} = \frac{\partial t}{\partial n} = 0 \tag{11}$$

with no variations in the direction n, orthogonal to the outflow boundary. Finally, on the free-stream boundary we can write:

$$v_\tau = |\mathbf{v}_\infty|; \quad v_n = \frac{\partial \omega}{\partial n} = \frac{\partial t}{\partial n} = 0 \tag{12}$$

where v_τ and v_n are the velocity components in the directions τ, tangential to the free-boundary, and n orthogonal to the free-boundary.

Temperature and mass fractions at interfaces

As already pointed out, convection in the fluid is effectively decoupled from conduction in the solid if the interface temperature is known a priori and is prescribed as a thermal boundary condition of the first kind. In such a case, under the additional assumption that the condensate is promptly removed, we have:

$$t = t_w \tag{13}$$

and the energy equation can be solved in the fluid region only (as it is done here).

In problems characterized by interface temperatures equation (13) lower than the dew-point, we use the ideal gas relationship to compute the value of the mass fraction of water vapor corresponding to the saturation pressure:

$$\omega_w = \frac{p_s(t_w)}{\rho R_v T_w} \tag{14}$$

In the above equation $p_s(t_w)$ is the saturation pressure at the wall temperature, R_v is the gas constant for water vapor, T_w is the absolute wall temperature, and the approximate relationship used to evaluate the saturation pressure is:

$$p_s = 610.78\, exp\left(17.2694 \frac{t}{t + 238.3}\right) \tag{15}$$

with P_s expressed in pascal and t expressed in degrees celsius (Comini *et al.*, 2005). Since, the wall temperature is known, equation (14) can be interpreted also as a boundary condition of the first kind for the mass fraction of water vapor.

Velocity components and mass fluxes at interfaces

At interfaces where condensation occurs, the usual no-slip boundary condition can still be prescribed in the direction tangential to the wall:

$$v_\tau = 0 \tag{16}$$

In the direction normal to the wall, on the contrary, velocity components assume the non-zero values which result from the mass balance illustrated in Appendix 2. Where condensation takes place, in fact, we obtain:

$$v_n = -\frac{\mathscr{D}}{1 - \omega_w} \frac{\partial \omega}{\partial n}\bigg|_w \tag{17}$$

for the component of the mass-average velocity of humid air orthogonal to the surface. Expressions (16) and (17) yield the velocity boundary conditions for the Navier-Stokes equations. Since, the boundary condition (17), the Navier-Stokes, the species conservation and the energy equations are coupled. On the other hand, if v_n is very small, as usually happens in air-conditioning processes, we can assume $v_n \cong 0$ and solve the governing equations independently of one another.

At surfaces where condensation takes place, we can express the total flux of water vapor as a sum of diffusive and advective components:

$$\dot{m}''_{\mathrm{v}} = (\dot{m}'')_{\mathrm{dv}} + (\dot{m}'')_{\mathrm{av}} = -\rho\mathscr{D}\frac{\partial\omega}{\partial n}\bigg|_{\mathrm{w}} + \rho\omega_{\mathrm{w}}v_{\mathrm{n}} \tag{18}$$

Thus, for $v_{\mathrm{n}} \cong 0$ the total flux can be expressed as:

$$\dot{m}''_{\mathrm{v}} \cong -\rho\mathscr{D}\frac{\partial\omega}{\partial n}\bigg|_{\mathrm{w}} = (\dot{m}'')_{\mathrm{dv}} \tag{19}$$

while, at surfaces where v_{n} is not negligible, the total flux can be expressed in the compact form:

$$\dot{m}''_{\mathrm{v}} = -\frac{\rho\mathscr{D}}{1-\omega_{\mathrm{w}}}\frac{\partial\omega}{\partial n}\bigg|_{\mathrm{w}} \tag{20}$$

which, in accordance with equations (17) and (18), takes into account both diffusion and advection components. In numerical simulations, the normal derivatives appearing in expressions (19) and (20) can be easily evaluated once a complete solution of the species conservation equation (3) has been obtained. In the framework of the finite element method, a convenient procedure of evaluation is described in Comini *et al.*(1995).

Sensible and latent heat fluxes

As already pointed out, numerical simulations assume that the humid air which comes into contact with the cooling surface is first brought to the wall temperature, and only afterwards is dehumidified until the final equilibrium state is reached. In psychrometric charts (which are usually based on a unit mass of dry air, and not on a unit mass of humid air), the process followed by the mixture can be represented as in Figure 1(a). (The relationship between x and ω is given by the expression:

$$x = \frac{\omega}{1-\omega} \tag{21}$$

which follows immediately from the respective definitions.)

The sensible heat exchange occurs first, with the moist air lowering its temperature from t_∞ to t_{w} while maintaining constant the value of the humidity ratio x_∞. The latent heat exchange follows, with the moist air lowering its humidity ratio from x_∞ to x_{w} while maintaining constant the value of the temperature t_{w}. If the condensate leaves the control volume of Figure 1(b) at the wall temperature t_{w}, the total rate of heat transfer from the humid air to the cooling surface can be expressed as (McQuinston *et al.*, 2005):

$$q_{\mathrm{w}} = \dot{m}_{\mathrm{a}}[\tilde{c}(t_\infty - t_{\mathrm{w}}) + H_{\mathrm{vl}}(t_{\mathrm{w}})(x_\infty - x_{\mathrm{w}})] \tag{22}$$

The energy balance in equation (22) paves the way to the consistent definitions of sensible:

$$q_k = \dot{m}_{\mathrm{a}}\tilde{c}_{\mathrm{p}}(t_\infty - t_{\mathrm{w}}) \tag{23}$$

and latent heat transfer loads:

$$q_\lambda = \dot{m}_{\mathrm{a}}H_{\mathrm{vl}}(t_{\mathrm{w}})(x_\infty - x_{\mathrm{w}}) = \dot{m}_{\mathrm{v}}H_{\mathrm{vl}}(t_{\mathrm{w}}) \tag{24}$$

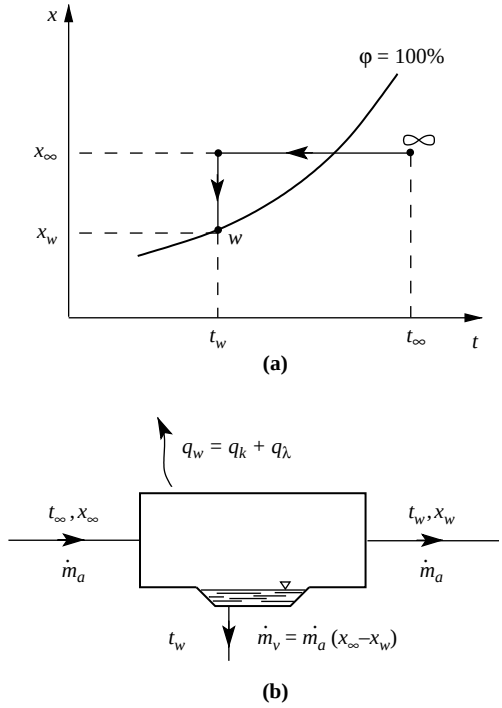

Figure 1.
Combined sensible and latent heat transfer: (a) process; (b) control volume schematization

In the above equations $\dot{m}_a$ is the mass flow rate of dry air, $\dot{m}_v$ is the mass flow rate of condensed vapor, $H_{vl}(t_w)$ is the latent heat of condensation, evaluated at the temperature t_w of the cooling surface, and:

$$\tilde{c}_p = c_{pa} + x c_{pv} \tag{25}$$

is the specific heat at constant pressure, evaluated at x_∞ and referred to a unit mass of dry air.

The sensible heat exchange is related to the conduction of heat from the wall to the fluid. Thus, in accordance with definition (23), numerical simulations assume:

$$q''_k = -k \left. \frac{\partial t}{\partial n} \right|_w \tag{26}$$

(It must be noted that the condensate leaves the domain at the reference temperature and, consequently, the contribution of this advective flow to the sensible heat exchange is identically equal to zero). The latent heat exchange is related to the condensation of water vapor. Definition (24) naturally leads to the assumption:

$$q''_\lambda = \dot{m}''_v H_{vl}(t_w) \tag{27}$$

which is utilized in numerical simulations for the evaluation of latent heat fluxes. In the above equation, the mass flux of water vapor is computed from equation (19)

in processes characterized by low rates of mass convection, or from equation (20) in processes characterized by high rates of mass convection. Finally, from equations (26) and (27) we have:

$$q''_{\mathrm{w}} = q''_{\mathrm{k}} + q''_{\lambda} = -k\left.\frac{\partial t}{\partial n}\right|_{\mathrm{w}} + \dot{m}''_{\mathrm{v}} H_{\mathrm{vl}}(t_{\mathrm{w}}) \tag{28}$$

for the total heat flux at the wall.

Heat and mass convection analogy

For the applications which are of interest here, the analogy between heat and mass convection can be written in the form:

$$\frac{Nu_{\mathrm{k}}}{Sh_{\mathscr{D}}} = \frac{1}{Le^{n}} \tag{29}$$

where the exponent n is equal to 1/3 in the laminar regime:

$$Nu_{\mathrm{k}} = \frac{q''_{\mathrm{k}} L}{k(t_{\infty} - t_{\mathrm{w}})} \tag{30}$$

is the Nusselt number related to the sensible heat exchange:

$$Sh_{\mathscr{D}} = \frac{(\dot{m}'')_{\mathrm{dv}} L}{\rho \mathscr{D}(\omega_{\infty} - \omega_{\mathrm{w}})} \tag{31}$$

is the Sherwood number related to the diffusive flux of water vapor, and:

$$Le = \frac{k}{\rho c_{\mathrm{p}}} \frac{1}{\mathscr{D}} = \frac{Sc}{Pr} \tag{32}$$

is the Lewis number, defined as the ratio between the Schmidt and the Prandtl numbers (Incropera and DeWitt, 1996).

Starting from the standard form of the convection analogy equation (29), and following the procedure of Appendix 3, the ratio between sensible and total heat fluxes can be expressed as:

$$\frac{q''_{\mathrm{k}}}{q''_{\mathrm{w}}} = \left[1 + Le^{n-1}(\omega_{\infty} - \omega_{w}) \frac{H_{\mathrm{vl}}(t_{\mathrm{w}})}{c_p(t_{\infty} - t_{\mathrm{w}})}\right]^{-1} \tag{33}$$

Equation (29) does not account for the advective transport of mass (Mills, 1999). Consequently, the validity of equations (29) and (33) is limited to processes characterized by low rates of mass convection, in which it is possible to assume: $v_{\mathrm{n}} \cong 0$ and $(\dot{m}'')_{\mathrm{dv}} \cong \dot{m}''_{\mathrm{v}}$.

On the contrary, in processes characterized by high rates of mass convection we have $v_{\mathrm{n}} \neq 0$, and the total flux of water vapor at the wall is expressed in compact form by equation (20), i.e. by the relationship:

$$\dot{m}'' v = \frac{1}{1 - \omega_{w}} (\dot{m}'')_{\mathrm{dv}} \tag{34}$$

which takes into account both diffusion and advection components of the mass flux. In this case, the Sherwood number related to the total wall flux of water vapor can be written as:

$$Sh_{\mathrm{w}} = \frac{\dot{m}''_{\mathrm{v}} L}{\rho \mathscr{D}(\omega_{\infty} - \omega_{\mathrm{w}})} = \frac{1}{1 - \omega_{\mathrm{w}}} Sh_{\mathscr{D}} \tag{35}$$

because of equation (34) and definition (31).

Substituting $(1 - \omega_{\mathrm{w}})Sh_{\mathrm{w}}$ for $Sh_{\mathscr{D}}$ into equation (29), we arrive at the modified form of the heat and mass convection analogy:

$$\frac{Nu_{\mathrm{k}}}{Sh_{\mathrm{w}}} = \frac{1 - \omega_{\mathrm{w}}}{Le^{n}} \tag{36}$$

valid for both low- and reasonably high-rates of mass convection. Starting from the modified form in equation (36) of the analogy, and following the steps illustrated in Appendix 3, the ratio between sensible and total heat fluxes can be expressed as:

$$\frac{q''_{\mathrm{k}}}{q''_{\mathrm{w}}} = \left[1 + Le^{n-1} \frac{\omega_{\infty} - \omega_{\mathrm{w}}}{1 - \omega_{\mathrm{w}}} \frac{H_{\mathrm{vl}}(t_{\mathrm{w}})}{c_p(t_{\infty} - t_{\mathrm{w}})}\right]^{-1} \tag{37}$$

Formula (37), but not expression (36), has been proposed by Volchkov *et al.* (2004). Obviously, it is only fair to notice that equation (37) implies equation (36), and vice versa.

Results and discussion

In the calculations, two sets of values were used for low- and high-rates of mass convection, respectively. In the low-rate range, we assumed: $t_{\mathrm{w}} = 10$°C and $\omega_{\mathrm{w}} = 0.00765$ at the interface with the cooling plate, while the constant values used for the thermophysical properties of humid air were: $\rho = 1.217\,\mathrm{kg/m^3}$, $\mu = 1.804 \times 10^{-5}\,\mathrm{N\,s/m^2}$, $\mathscr{D} = 2.45 \times 10^{-5}\,\mathrm{m^2/s}$, $c_p = 1.027\,\mathrm{kJ/(kg\ K)}$, $k = 2.566 \times 10^{-2}\,\mathrm{W/(m\ K)}$, $H_{\mathrm{vl}} = 2{,}478\,\mathrm{kJ/kg}$, $Sc = 0.605$, $Pr = 0.722$ and $Le = Sc/Pr = 0.838$. In the high-rate range, we assumed: $t_{\mathrm{w}} = 60$°C and $\omega_{\mathrm{w}} = 0.13236 = 0$ at the interface with the cooling plate, while the constant values used for the thermophysical properties of humid air were: $\rho = 1.207\,\mathrm{kg/m^3}$, $\mu = 1.910 \times 10^{-5}\,\mathrm{N\,s/m^2}$, $\mathscr{D} = 2.45 \times 10^{-5}\,\mathrm{m^2/s}$, $c_p = 1.332\,\mathrm{kJ/(kg\ K)}$, $k = 2.833 \times 10^{-2}\,\mathrm{W/(m\ K)}$, $H_{\mathrm{vl}} = 2{,}362\,\mathrm{kJ/kg}$, $Sc = 0.646$, $Pr = 0.898$ and $Le = Sc/Pr = 0.719$.

Simultaneous heat and mass transfer: analytical results

The analytical results deal with the range of validity of the two forms in equations (33) and (37) of the heat and mass convection analogy. In the literature, in fact, there is not much agreement on the definition of the limits for the "low" and "high" rates of mass-convection. However, a "safe" criterion can be seen from Figure 2 where the results yielded by equations (33) and (37) are compared. In Figure 2(a), the standard and the modified form of the analogy yield undistinguishable results. Thus, with a wall temperature $t_{\mathrm{w}} = 10$°C, the limits: $t_{\infty} < 60$°C, for free-stream temperatures, and $\Delta\omega = \omega_{\infty} - \omega_{\mathrm{w}} < 0.045$, for mass fraction differences, can be assumed for the low range (in which the standard form of the analogy and the related boundary condition $v_{\mathrm{n}} = 0$ hold well). On the contrary, in Figure 2(b) the standard and the modified form of the analogy

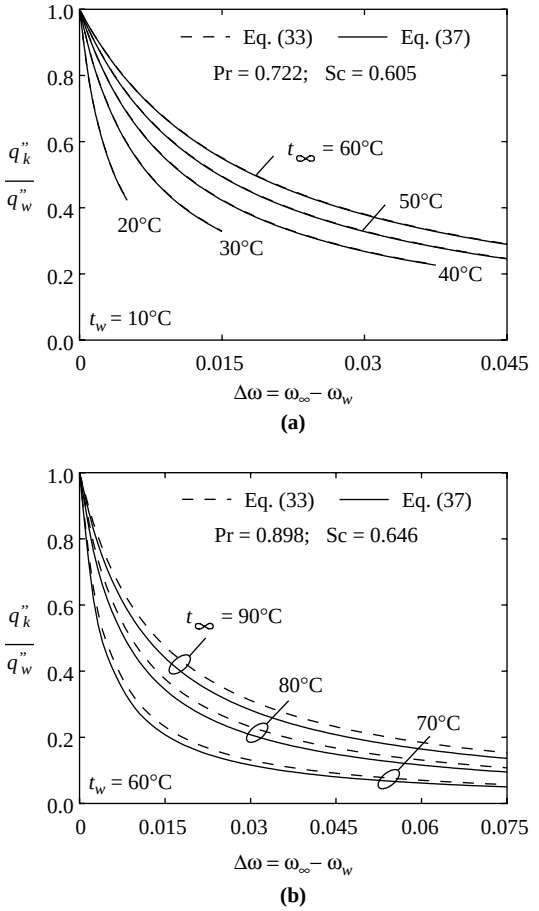

Figure 2.
Results yielded by the standard form of the analogy (33) and the modified form of the analogy (37) for (a) low and (b) high rates of mass convection

yield results which differ as much as 15 percent. Thus, with a wall temperature $t_w = 60°C$, the limits: $70°C < t_\infty < 90°$ for free-stream temperatures and $\Delta\omega = \omega_\infty - \omega_w < 0.075$ for mass fraction differences can be assumed for the high range (in which the modified form of the analogy and the related boundary condition $v_n \neq 0$ must be used).

Simultaneous heat and mass transfer: numerical results

The numerical results deal with the validation of the model utilized for the prediction of heat and mass fluxes under dehumidifying conditions. In the numerical solutions we utilized the commercial code FEMLAB (COMSOL, 2004) and, in the high-range of mass convection, also an iterative solution procedure. In the iterative calculations we assumed, at the first step, negligible advective velocities at the wall boundary. Then we computed in sequence the velocity field, the temperature field and the mass fraction field. The computed distribution of mass fraction gradients yielded non-zero estimates

of advective velocity distributions, which were used to repeat the calculations until convergence was reached. After obtaining a converged solution, the computed gradients of temperature and mass fractions at the walls were used to estimate latent, sensible and total heat fluxes.

The computational domain, the grid and the boundary conditions utilized in the calculations are shown in Figure 3. The domain, of length $L = 0.1\,\text{m}$ and width $W = 0.05\,\text{m}$, is subdivided into quadratic triangular elements. Grid and time-step independence were established on the basis of calculations in which the dimensions of the elements and the time step were progressively reduced from one simulation to another. When further decreases in dimensions, or in time steps, led to changes in the average Nusselt numbers smaller than 1 percent, the results were considered to be independent on the grid, or on the time step, respectively. The final grid consisted of 4,019 elements with a total of 8,516 nodes. Grid spacings were finer near the wall and the leading edge, and the final value of the time step was equal to 0.6 s.

In Figure 4 the analytical results yielded by the modified form of the heat and mass transfer analogy of equation (37) are compared with the steady-state results of numerical calculations concerning several Reynolds numbers in the range ($(5 \times 10^3 \leq Re_L \leq 1 \times 10^5)$). In Figure 4(a) the numerical results are shown using the boundary condition $v_n = 0$, while in Figure 4(b) the numerical results are shown using the boundary condition (17). As can be seen, the agreement is quite good both for the low-rates of mass convection shown in Figure 4(a), and the high-rates of mass convection shown in Figure 4(b). Furthermore, the independence of the ratios q''_k/q''_w on the Reynolds number, implied by the heat and mass convection analogy, is confirmed. In fact results concerning low and high Reynolds number results are practically indistinguishable in both figures.

Simultaneous heat and mass transfer: future developments

In design procedures, once the ratios between sensible and total heat loads have been evaluated on the basis of the heat and mass convection analogy, either the sensible or

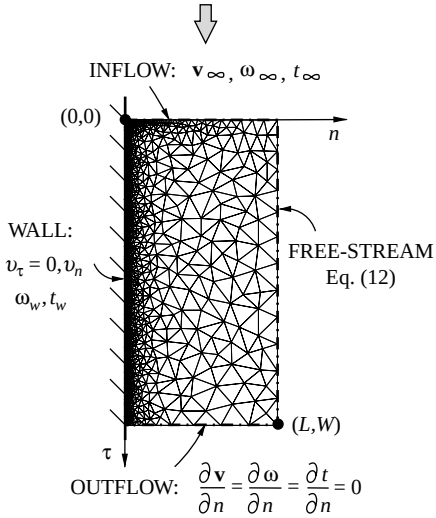

Figure 3.
Computational domain, grid and boundary conditions

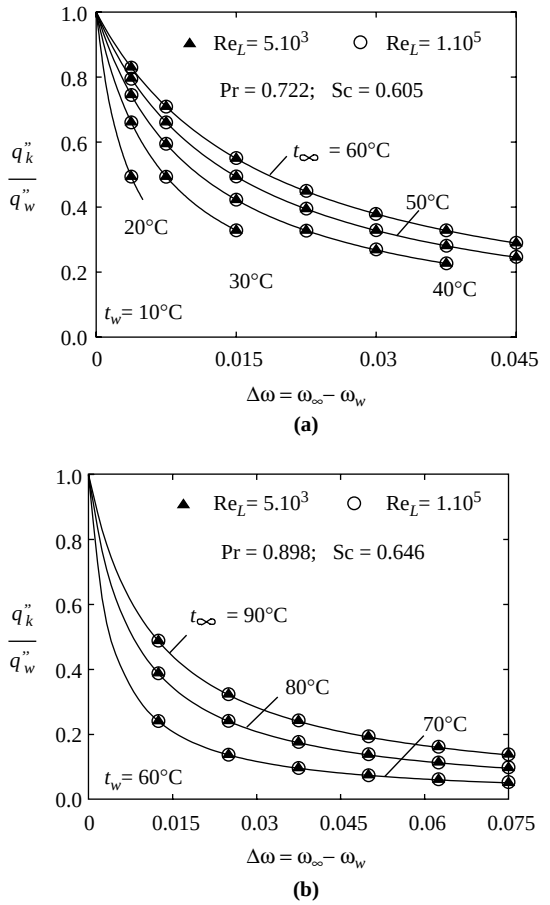

Figure 4.
Comparisons between analytical (continuous) results yielded by the modified form of the analogy and finite element results for (a) low and (b) high rates of mass convection

the total heat flow rate must still be calculated. In processes with low-rates of mass convection, the influence of the advective velocities v_n can be neglected, and sensible heat flow rates can be evaluated by means of standard expressions correlating the average Nusselt number with the Reynolds and Prandtl numbers. In processes with high-rates of mass convection, on the contrary, the influence of v_n must be taken into account. To this aim, some indications can be obtained from the data base provided by the numerical calculations illustrated in the previous section.

In the cold-plate problem investigated here the flow is laminar, and boundary conditions of constant and uniform temperature and mass fraction are imposed at the interface between solid and fluid domains. Under these assumptions, the ratio $\overline{Nu}_k/(\overline{Nu}_k)_0$ between the actual average Nusselt number and the average Nusselt number for small, in the limit zero, advective velocities v_n can be expressed as a function of the flow parameter $(\bar{v}_n/|\mathbf{v}_\infty|)\,\mathrm{Re}_L^{1/2}$ (Eckert and Drake, 1959; Hartnett, 1985). (Here, the average Nusselt number:

$$\overline{Nu}_{\mathrm{k}} = \left(\frac{1}{A}\int_0^A q''_{\mathrm{k}}\,\mathrm{d}A\right)\frac{L}{k(t_\infty - t_{\mathrm{w}})} = \frac{q_k L}{Ak(t_\infty - t_{\mathrm{w}})} \tag{38}$$

and the average advective velocity:

$$\bar{v}_{\mathrm{n}} = \frac{\dot{m}_{\mathrm{v}}}{\rho_{\mathrm{v}} A} \tag{39}$$

are defined with reference to the total values of the exchange area A, sensible heat flow rate q_{k}, and mass flow rate of condensing vapor $\dot{m}_{\mathrm{v}}$). In this way, the plot of Figure 5 shows the almost linear correlation:

$$\frac{\overline{Nu}_{\mathrm{k}} - (\overline{Nu}_{\mathrm{k}})_0}{(\overline{Nu}_{\mathrm{k}})_0} \cong 9.7\,\frac{|\bar{v}_{\mathrm{n}}|}{|\mathbf{v}_\infty|}\,Re_L^{1/2} \tag{40}$$

which is characterized by an accuracy of the order of 2 percent in the whole range of the $(\bar{v}_{\mathrm{n}}/|\mathbf{v}_\infty|)Re_L^{1/2}$ parameter investigated here.

Conclusions

A joint description of heat and mass transfer and thermodynamic aspects of air-cooling applications has been presented, based on the boundary conditions utilized in numerical simulations. Particular attention has been paid to the thermodynamically consistent definition of latent and sensible heat loads, and to the correct formulation of the heat and mass transfer analogy in the presence of a suction flow induced by condensation of water vapor.

In the model illustrated in the text, conduction in the solid and convection in the fluid have been decoupled by imposing constant temperature boundary conditions on the interface, and by assuming that the condensate is promptly removed. However, for high rates of mass convection the condensation of water vapor induces non-zero advective velocities on the exchange surface, modifying the flow field and influencing also the species and the energy conservation equations. Consequently, the equations governing heat and mass transfer in the fluid are coupled with the Navier-Stokes equations, and the solution must be based on an iterative procedure.

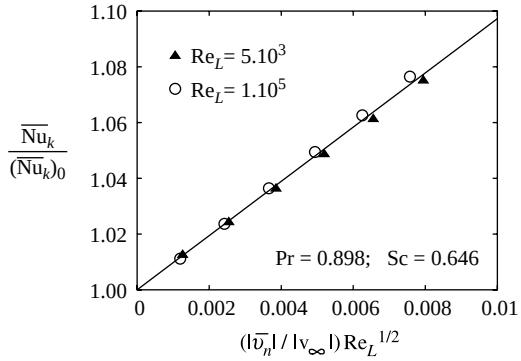

Figure 5.
Laminar flow of humid air over a cooling plate: ratio of the actual Nusselt number to the Nusselt number with very small advective velocities v_{n}

The high-rates of mass convection required also a modification of the analogy between heat and mass convection. The predictions of the modified analogy were satisfactorily compared with the numerical results concerning forced flows of humid air over a cooled plate. In this way the model utilized for the simulations was validated, both for air-conditioning applications (almost always characterized by low rates of mass convection), and drying applications (almost always characterized by high-rates of mass convection).

The proposed methodology leaves room for further research. In particular, the effects on the Nusselt number of the suction flow induced by condensation must be quantified. To this aim, some indications have been provided in the text for the cold-plate problem investigated here.

References

Bari, E., Noel, J.Y., Comini, G. and Cortella, G. (2005), "Air-cooled condensing systems for home and industrial appliances", *Applied Thermal Engineering*, Vol. 25, pp. 1446-58.

Comini, G. (2000), *Fundamentals of Applied Thermodynamics*, SGE Editoriali, Padova, (in Italian).

Comini, G. and Cortella, G. (2005), *Fundamentals of Heat Transfer*, SGE Editoriali, Padova, (in Italian).

Comini, G. and Croce, G. (2001), "Convective heat and mass transfer in tube-fin exchangers under dehumidifying conditions", *Numerical Heat Transfer, Part A*, Vol. 40, pp. 579-99.

Comini, G. and Croce, G. (2003), "Numerical simulation of convective heat and mass transfer in banks of tubes", *International Journal for Numerical Methods in Engineering*, Vol. 57, pp. 1755-73.

Comini, G., Cortella, G. and Manzan, M. (1995), "A streamfunction-vorticity based finite-element formulation for laminar-convection problems", *Numerical Heat Transfer, Part B*, Vol. 28, pp. 1-22.

Comini, G., Nonino, C. and Savino, S. (2002), "Convective heat and mass transfer in wavy finned-tube exchangers", *International Journal of Numerical Methods for Heat & Fluid Flow*, Vol. 12, pp. 735-55.

Comini, G., Nonino, C. and Savino, S. (2005), "Convective heat and mass transfer under dehumidifying conditions", in Bennacer, R. (Ed.), *Progress in Computational Heat and Mass Transfer*, Vol. II, Editions TEC & DOC - Lavoisier, Paris, Invited lecture, pp. 711-22.

COMSOL (2004), *FEMLAB User's Guide*, COMSOL AB, Stockholm, Version 3.0.

Eckert, E.R.G. and Drake, R.M. (1959), *Chapter 16: Mass transfer, in Heat and Mass Transfer*, McGraw-Hill, New York, NY.

Galvin, K.P. (2005), "A conceptually simple derivation of the Kelvin equation", *Chemical Engineering Science*, Vol. 60, pp. 4659-60.

Hartnett, J.P. (1985), "Chapter 1: Mass transfer cooling", in Rohsenow, W.M., Hartnett, J.P. and Ganic, E.N. (Eds), *Handbook of Heat Transfer*, 2nd ed., McGraw-Hill, New York, NY.

Hartnett, J.P. and Eckert, E.R.G. (1957), "Mass transfer cooling in a laminar boundary layer with constant fluid properties", *Trans. ASME, Series C*, Vol. 79, pp. 247-54.

Hu, X., Zhang, L. and Jacobi, A.M. (1994), "Surface irregularity effects of droplets and retained condensate on local heat transfer to finned tubes in cross-flow", *ASHRAE Transactions*, Vol. 118-1, pp. 375-81.

Incropera, F.P. and DeWitt, D.P. (1996), *Fundamentals of Heat and Mass Transfer*, 4th ed., Wiley, New York, NY.

Korte, C. and Jacobi, A.M. (2001), "Condensate retention effects on the performance of plain-fin-and-tube heat exchangers: retention data and modeling", *Journal of Heat transfer*, Vol. 123, pp. 926-36.

Kuehn, T.H., Ramsey, J.W. and Threlkeld, J.L. (1998), *Thermal Environmental Engineering*, Prentice-Hall, Upper Saddle River, NJ.

McQuinston, F.C. (1975), "Fin efficiency with combined heat and mass transfer", *ASHRAE Transactions*, Vol. 81 No. 1, pp. 350-5.

McQuinston, F.C., Parker, J.D. and Spitler, J.D. (2005), *Heating, Ventilating and Air Conditioning - Analysis and Design*, 6th ed., Wiley, New York, NY.

Mills, A.F. (1999), *Basic Heat & Mass Transfer*, Prentice-Hall, Upper Saddle River, NJ.

Mitrovic, J. (2004), "On the equilibrium conditions of curved interfaces", *International Journal of Heat and Mass transfer*, Vol. 47, pp. 809-18.

Na, B. and Webb, R.L. (2004), "A fundamental understanding of factors affecting frost nucleation", *International Journal of Heat and Mass Transfer*, Vol. 46, pp. 3798-808.

Ramadhyani, S. (1998), "Chapter 6: Calculation of air-side heat transfer in compact heat exchangers under condensing conditions", in Sunden, B. and Faghri, M. (Eds), *Computer Simulations in Compact Heat Exchangers*, Computational Mechanics Publications, Southampton.

Spahier, L.A. and Worek, W.M. (2004), "Analysis of heat and mass transfer in porous sorbents used in rotary regenerators", *International Journal of Heat and Mass transfer*, Vol. 47, pp. 3415-30.

Volchkov, E.P., Terekhov, V.V. and Terekhov, V.I. (2004), "A numerical study of boundary-layer heat and mass transfer in a forced flow of humid air with surface steam condensation", *International Journal of Heat and Mass Transfer*, Vol. 47, pp. 1473-81.

Wallace, J.M. and Hobbes, P.H. (1977), *Atmospheric Science: An Introductory Survey*, Academic Press, New York, NY.

Appendix 1. Kelvin equation and surface roughness

At a temperature T, the saturation pressure P_0 of a liquid is the vapor pressure measured just above a planar interface but, when the interface exhibits a curvature, the equilibrium vapor pressure P_v becomes higher than P_0. A simple derivation of the relationship between the two pressures can follow the steps outlined in Galvin (2005). With reference to a system containing liquid water and water vapor in equilibrium at the temperature T, let us assume that a capillary tube with a non-wetting surface is inserted into the liquid as shown in Figure A1(a). In such a case, the liquid moves downwards in the capillary, and the depression:

$$\Delta h = \frac{1}{\rho_l g}\,\frac{2\sigma}{r} \tag{A1}$$

depends on the liquid density ρ_l, the surface tension σ, the gravity acceleration g and the capillary radius r. Equation (A1) can also be written in the form:

$$g\Delta h = \frac{1}{\rho_l}\,\frac{2\sigma}{r} = \Delta G \tag{A2}$$

where G is the chemical potential (Mitrovic, 2004). The three members of equation (A2) have the dimension of a specific energy (J/m^3), and represent the energy per unit mass required to overcome the Gibbs energy barrier in order to form the surface of the vapor-liquid interface (Na and Webb, 2004).

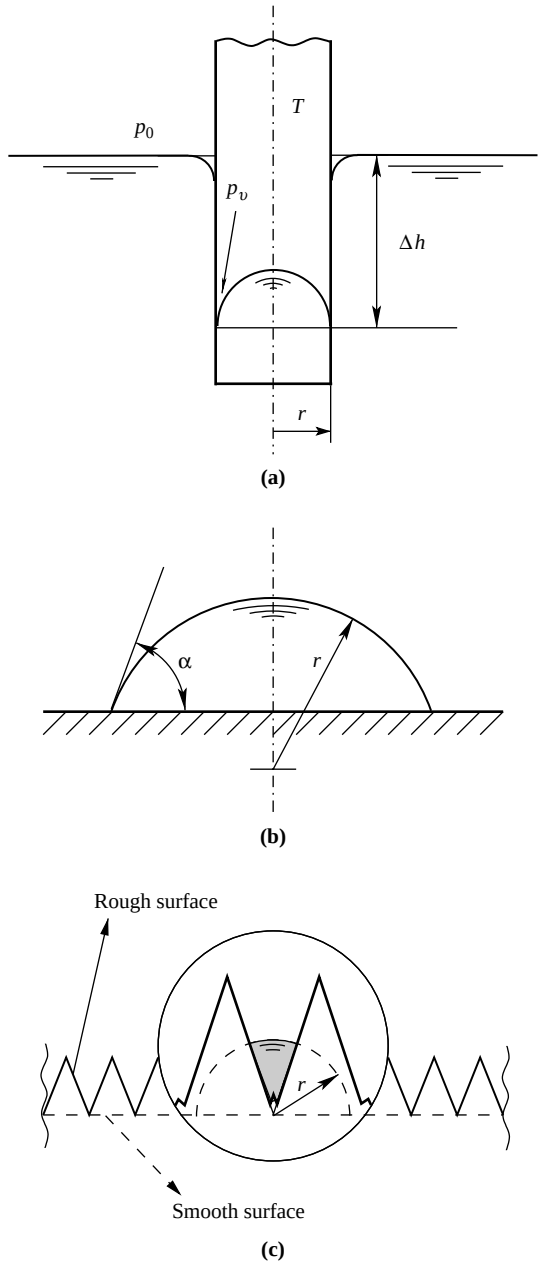

Figure A1.
Influence of (a) radius of curvature; (b) contact angle; (c) surface roughness

Inside the capillary the temperature is constant and, consequently, the pressure gradient can be written as:

$$\left(\frac{\partial p}{\partial h}\right)_T = \rho_v g = \frac{p}{R_v T} g \tag{A3}$$

Separating the variables and integrating the first and the third member of equation (A3) from the limits (P_0, 0) and (p_v, Δh), we obtain:

$$\ln \frac{p_v}{p_0} = \frac{g \Delta h}{R_v T} \tag{A4}$$

Finally, by taking into account the first two members of equation (A2), we arrive at the usual expression of the Kelvin equation:

$$\frac{p_v}{p_0} = \exp\left(\frac{1}{R_v T \rho_l} \frac{2\sigma}{r}\right) \tag{A5}$$

On the basis of the Clausius-Clapeyron relation, the first member of equation (A4) can also be written in the form (Comini, 2000):

$$\ln \frac{p_v}{p_0} = \frac{H_{lv}}{R_v} \left(\frac{1}{T_0} - \frac{1}{T_v}\right) \tag{A6}$$

where T_0 is the saturation temperature at the pressure P_0 and T_v is the saturation temperature at the pressure P_v. Thus, by equating the second members of equations (A4) and (A6), after some algebra we arrive at the expression:

$$\frac{T_v - T_0}{T_0} = \frac{1}{\rho_l H_{lv}} \frac{2\sigma}{r} \tag{A7}$$

of the sub-cooling required to form an interface of radius r in the situation of Figure A1(a), or a droplet of radius r in a humid air-stream. From equation (A7) it stems that the required sub-cooling increases with the curvature. As a consequence, it is not likely that homogeneous nucleation occurs within a humid air-stream. On the other hand, water droplets forming on nuclei of condensation have much less curvature in relation to their masses. In the atmosphere, in fact, heterogeneous nucleation on foreign particles occurs worldwide and leads to the formation of clouds (Wallace and Hobbes, 1977). As shown in Figures A1(b) and (c), also water droplets forming on wetting ($\alpha < 180°$) and rough surfaces may have much less curvature with respect to spherical droplets with the same masses. Consequently, the appearance of condensation on the wall surfaces may occur with much smaller degrees of sub-cooling than the corresponding formation of spherical droplets within the humid air-stream.

Appendix 2. Mass balances at the interface

In the direction n, the boundary conditions for the component v_n of the mixture velocity **v** must take into account the mass balances. The species conservation equation (3) implies that the diffusive flux of water vapor at an interface can be expressed by equation (19):

$$(\dot{m}'')_{dv} = -\rho \mathcal{D} \left.\frac{\partial \omega}{\partial n}\right|_{n=0}$$

while the advective flux of water vapor can be expressed as:

$$(\dot{m}'')_{\mathrm{av}} = \rho\omega_{\mathrm{w}} v_{\mathrm{n}} \tag{A8}$$

The total flux of water vapor can be expressed by the sum of equation (18):

$$\dot{m}''_{\mathrm{v}} = (\dot{m}'')_{\mathrm{dv}} + (\dot{m}'')_{\mathrm{av}} = -\rho\mathscr{D}\frac{\partial\omega}{\partial n}\bigg|_{n=0} + \rho\omega_{\mathrm{w}} v_{\mathrm{n}}$$

With reference to Figure A2, we can see that the mass fraction of dry-air in the humid-air mixture is equal to $(1 - \omega)$ and, consequently, the advective flux of dry air at the interface is equal to:

$$(\dot{m}'')_{\mathrm{aa}} = \rho(1 - \omega_{\mathrm{w}}) v_{\mathrm{n}} \tag{A9}$$

The diffusive flux of dry air at the interface is obtained by substituting ω with $(1 - \omega)$ in equation (19). In this way we arrive at the expression:

$$(\dot{m}'')_{\mathrm{da}} = -\rho\mathscr{D}\frac{\partial(1-\omega)}{\partial n}\bigg|_{n=0} = \rho\mathscr{D}\frac{\partial\omega}{\partial n}\bigg|_{n=0} \tag{A10}$$

Since, the wall is not permeable to dry air, the total flux of dry air at the interface must be set equal to zero:

$$\dot{m}''_{\mathrm{a}} = (\dot{m}'')_{\mathrm{da}} + (\dot{m}'')_{\mathrm{aa}} = \rho\mathscr{D}\frac{\partial\omega}{\partial n}\bigg|_{n=0} + \rho(1 - \omega_{\mathrm{w}}) v_{\mathrm{n}} = 0 \tag{A11}$$

Equation (A11) yields the unknown advective velocity:

$$v_{\mathrm{n}} = -\frac{\mathscr{D}}{1 - \omega_{\mathrm{w}}}\frac{\partial\omega}{\partial n}\bigg|_{n=0}$$

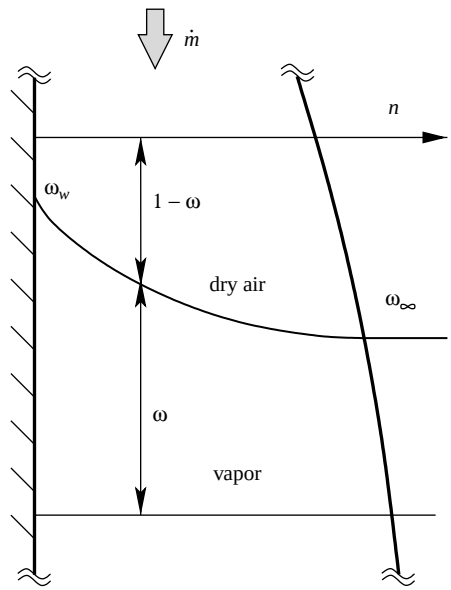

Figure A2.
Diffusion of water vapor through air

i.e. the boundary condition (17) for the normal component of the mass-average velocity of humid air at a boundary where condensation takes place.

Finally, by substituting equation (17) into equation (18) we obtain:

$$\dot{m}''_{\mathrm{v}} = -\rho\mathscr{D}\left(1+\frac{\omega_{\mathrm{w}}}{1-\omega_{\mathrm{w}}}\right)\left.\frac{\partial\omega}{\partial n}\right|_{n=0} = -\frac{\rho\mathscr{D}}{1-\omega_{\mathrm{w}}}\left.\frac{\partial\omega}{\partial n}\right|_{\mathrm{w}}$$

i.e. the expression (20) of the total flux of water vapor at a boundary where condensation takes place.

Appendix 3. Ratio of sensible and total heat fluxes

The ratio between total and sensible heat fluxes can be written as:

$$\frac{q''_{\mathrm{w}}}{q''_{\mathrm{k}}} = 1+\frac{q''_{\lambda}}{q''_{\mathrm{k}}} = 1+\frac{\dot{m}''_{\mathrm{v}}H_{\mathrm{vl}}(t_W)}{q''_{\mathrm{k}}} \tag{A12}$$

and the modified form, equation (36) of the heat and mass convection analogy can be written as:

$$\frac{Sh_{\mathrm{w}}}{Nu_{\mathrm{k}}} = \frac{\dot{m}''_{\mathrm{v}}L}{\rho\mathscr{D}(\omega_{\infty}-\omega_{\mathrm{w}})}\,\frac{k(t_{\infty}-t_{\mathrm{w}})}{q''_{\mathrm{k}}L} = \frac{1}{1-\omega_{\mathrm{w}}}Le^{n} \tag{A13}$$

equation (A13) leads to the expression:

$$\frac{\dot{m}''_{\mathrm{v}}}{q''_{\mathrm{k}}} = Le^{n}\,\frac{\omega_{\infty}-\omega_{\mathrm{w}}}{1-\omega_{\mathrm{w}}}\,\mathscr{D}\,\frac{\rho c_p}{k}\,\frac{1}{c_p(t_{\infty}-t_{\mathrm{w}})} \tag{A14}$$

for the ratio between the mass flux of water vapor and the total flux of heat at the wall. Noting that $\mathscr{D}\rho c_p/k = Le-1$ and substituting equation (A14) into equation (A12) we arrive at the relationship:

$$\frac{q''_{\mathrm{w}}}{q''_{\mathrm{k}}} = 1+Le^{n-1}\frac{\omega_{\infty}-\omega_{\mathrm{w}}}{1-\omega_{\mathrm{w}}}\,\frac{H_{\mathrm{vl}}(t_{\mathrm{w}})}{c_p(t_{\infty}-t_{\mathrm{w}})} \tag{A15}$$

Taking the reciprocal of both members of equation (A15) we finally arrive at equation (37). Starting from the expression (29) of the heat and mass convection analogy, and following the steps just outlined we arrive at equation (33).

Corresponding author

G. Comini can be contacted at: gianni.comini@uniud.it

To purchase reprints of this article please e-mail: **reprints@emeraldinsight.com**
Or visit our web site for further details: **www.emeraldinsight.com/reprints**